

# Population Pharmacokinetics of Glasdegib in Patients With Advanced Hematologic Malignancies and Solid Tumors

The Journal of Clinical Pharmacology  
2020, 60(5) 605–616  
© 2019 Pfizer Inc. The *Journal of Clinical Pharmacology* published by Wiley Periodicals, Inc. on behalf of American College of Clinical Pharmacology  
DOI: 10.1002/jcph.1556

Swan Lin, PharmD<sup>1</sup>, Naveed Shaik, PhD<sup>1</sup>, Giovanni Martinelli, MD<sup>2</sup>, Andrew J. Wagner, MD, PhD<sup>3</sup>, Jorge Cortes, MD<sup>4</sup>, and Ana Ruiz-Garcia, PharmD, PhD<sup>1</sup>

## Abstract

Glasdegib is an inhibitor of the Hedgehog pathway recently approved in the United States for the treatment of acute myeloid leukemia. A population pharmacokinetic analysis was conducted to characterize the kinetic behavior of glasdegib and its sources of variability (covariates) by utilizing data from 269 patients with cancer treated with oral glasdegib doses ranging from 5 to 640 mg/d. Nonlinear mixed-effects modeling was conducted using NONMEM (v.7.3) and Perl-speaks NONMEM (v.4.2.0). The estimated apparent total clearance, apparent central volume of distribution, and apparent peripheral volume of distribution were 6.27 L/h, 3.32 L, and 279.2 L, respectively. Age, sex, race, and hepatic function were not significant covariates on glasdegib pharmacokinetic parameters. Baseline body weight, percentage bone marrow blasts, creatinine clearance, and use of moderate or strong cytochrome P450 3A inhibitors were statistically significant covariates on apparent total clearance; however, the magnitude of the effects was not considered clinically meaningful.

## Keywords

acute myeloid leukemia, Hedgehog, myelodysplastic syndrome, population pharmacokinetics, Smoothened inhibitor

Glasdegib (PF-04449913), an oral, small-molecule inhibitor of the Smoothened (SMO) receptor, selectively inhibits the Hedgehog signaling pathway. Glasdegib has been evaluated in patients with cancer with hematologic malignancies and solid tumors in monotherapy dose-escalation studies over the dose range of 5 to 640 mg once daily (QD).<sup>1–3</sup> In the first-in-human dose-escalation study, the maximum tolerated dose (MTD) of glasdegib was 400 mg QD, and the maximum administered dose was 600 mg QD.<sup>1</sup> Based on evidence of consistent downregulation of the Hedgehog pathway at  $\geq 100$  mg QD, initial clinical efficacy signals, and safety and tolerability evaluation, a dose of  $\leq 200$  mg QD was selected as the recommended phase 2 dose. Further, due to the expected long-term drug administration, and to provide additional safety margin for potential drug-drug interactions (DDI) that may increase glasdegib exposure, the 100 mg QD dose was chosen for further clinical evaluation. Glasdegib at the clinical dose of 100 mg QD is currently under evaluation in combination with chemotherapy in patients with acute myeloid leukemia (AML) or high-risk myelodysplastic syndrome (MDS).<sup>4,5</sup> Glasdegib was recently approved in the United States for the treatment of AML in elderly patients or patients with comorbidities that exclude the use of intensive induction chemotherapy.<sup>6</sup>

Data from noncompartmental pharmacokinetic (PK) analysis for glasdegib administered to patients with hematologic malignancies indicated dose-

proportional increase in plasma exposure (5–600 mg QD) following single and multiple daily dosing.<sup>1</sup> The mean plasma elimination half-life of glasdegib across the dose levels tested ranged from 17.4 to 34.3 hours. The median observed accumulation ratio in glasdegib-treated patients ranged from 1.2 to 2.5 and was consistent with the observed plasma half-life of the drug. In healthy subjects glasdegib PK was not affected in a clinically relevant manner by a high-fat meal or by use of proton pump inhibitors.<sup>7</sup>

Glasdegib has high absolute oral bioavailability (77.12%) and is extensively distributed.<sup>1,8</sup> Glasdegib is eliminated primarily by oxidative metabolism, mostly

<sup>1</sup>Clinical Pharmacology, Global Product Development, Pfizer Inc, San Diego, California, USA

<sup>2</sup>Istituto Scientifico Romagnolo per lo Studio e la Cura dei Tumori (IRST IRCCS), Meldola, Italy

<sup>3</sup>Dana-Farber Cancer Institute, Boston, Massachusetts, USA

<sup>4</sup>University of Texas MD Anderson Cancer Center, Houston, Texas, USA

This is an open access article under the terms of the Creative Commons Attribution-NonCommercial-NoDerivs License, which permits use and distribution in any medium, provided the original work is properly cited, the use is non-commercial and no modifications or adaptations are made.

Submitted for publication 30 August 2019; accepted 22 October 2019.

## Corresponding Author:

Swan Lin, PharmD, Clinical Pharmacology, Global Product Development, Pfizer Inc, 10555 Science Center Dr (CB10/002/2408B), San Diego, CA 92121

Email: swan.lin@pfizer.com

by cytochrome P450 (CYP) 3A4, with minor contribution from glucuronidation by uridine diphosphate glucuronosyltransferase 1A9. The plasma exposures of glasdegib were increased by a strong CYP3A inhibitor<sup>9</sup> and decreased by a strong CYP3A4 inducer.<sup>8</sup> In a radiolabel mass balance study, a mean of 48.9% and 41.7% of the radiolabeled dose was recovered in urine and feces, respectively. Unchanged glasdegib recovered in the urine and feces accounted for 17.2% and 19.5% of the 100 mg dose.<sup>10</sup>

The objectives of this analysis were to develop a PK model to characterize glasdegib kinetic behavior and to determine the sources of variability in glasdegib PK parameters through covariate analysis.

## Methods

### Clinical Studies

Patient data were included from 3 glasdegib studies (ClinicalTrials.gov identifier): B1371001 (NCT00953758), B1371002 (NCT01286467), and B1371003 (NCT01546038). All studies were approved by independent ethics committees and conducted in accordance with the Declaration of Helsinki and Good Clinical Practice. All subjects and patients provided written, informed consent for participation. The study sites and institutional review boards for each trial are provided in Supplemental Table S1.

In study B1371001, patients with hematologic malignancies received oral glasdegib 5, 10, 20, 40, 80, 120, 180, 270, 400, or 600 mg QD as monotherapy. B1371002 was a dose-ranging study in patients with solid tumors treated with glasdegib 80, 160, 320, or 640 mg QD as monotherapy. B1371003 was a phase 1b/2 study in patients with AML and high-risk MDS. In the phase 1b portion, glasdegib was administered at 2 dose levels, 100 mg or 200 mg QD, with either low-dose cytarabine, decitabine, or a chemotherapy regimen of 7 days of standard-dose cytarabine and 3 days of an anthracycline (7+3). In the phase 2 portion of B1371003, in a subset of the patients considered ineligible to receive intensive chemotherapy ( $n = 132$ ), low-dose cytarabine was administered with versus without glasdegib 100 mg QD. In the subset of patients eligible for intensive chemotherapy ( $n = 71$ ), the 7+3 regimen was administered with versus without glasdegib. For studies B1371001 and B1371002, glasdegib was administered in the fasted state, and in B1371003 glasdegib was administered without regard to food.

### PK Assessment

Intensive sampling for single-dose glasdegib PK was available for studies B1371001 (predose, 0.5, 1, 2, 4, 8, 24, 48, 96, and 120 hours) and B1371002 (predose, 1, 2, 4, 6, 10, and 24 hours). Only sparse sampling for single-dose glasdegib was available for study B1371003.

For multiple-dose PK analysis, intensive sampling was collected from all 3 studies. Details on the sample collection are shown in Supplemental Table S2.

Plasma samples were analyzed for glasdegib concentrations using a validated, sensitive, and specific high-performance liquid chromatography–tandem mass spectrometry method.<sup>10</sup> No values were below the lower limit of quantitation for glasdegib (0.200 ng/mL). Missing glasdegib concentration values were excluded from the data set.

### Structural Model Development

The analysis was performed using nonlinear mixed-effects modeling methodology in NONMEM version 7.3.0 (ICON Development Solutions, Ellicott City, Maryland). Stochastic approximation expectation-maximization/Monte Carlo importance sampling was used. This integrates the posterior density by performing a Monte Carlo sampling over the parameters during the expectation step and then uses a single iteration maximization step in order to advance the fixed-effect parameters toward the maximum likelihood.<sup>11</sup> Interindividual variability (IIV) in the PK parameters was modeled using multiplicative exponential random effects ( $\omega^2$ ). Residual variability was modeled using a proportional error model with log-transformed glasdegib plasma concentrations and thetazitized sigma.

Structural models, including 1-compartment or 2-compartment models and different absorption models (0- and first-order absorption models, evaluation of lag time, mixed absorption models, and transit compartment absorption models), were explored. Model selection was based on change in objective function value (OFV), visual inspection of diagnostic plots, model stability, precision of the parameter estimates, and decreases in variability. A 2-compartment model best described the data and included the following parameters: apparent total clearance (CL/F), apparent central volume of distribution (Vc/F), apparent peripheral volume of distribution (Vp/F), intercompartmental clearance (Q/F), and first-order absorption rate constant ( $k_a$ ).

### Covariate Analyses

Potential covariates were selected and tested for significance by stepwise covariate modeling as implemented in Perl-speaks-NONMEM version 4.2.0.<sup>12</sup> Forward inclusion to the full model was based on statistical criterion  $\alpha = 0.05$ , and backward elimination for the final model was based on the criterion  $\alpha = 0.001$ .

Demographic covariates (baseline body weight, baseline age, sex, and race), baseline laboratory tests (eg, weight-standardized creatinine clearance [CR<sub>CL</sub>], aspartate transaminase, total bilirubin, albumin,

**Table 1.** Covariates Evaluated on Population Pharmacokinetic Base Model

PK Parameter	Covariate
CL/F	Age, WNCL <sup>a</sup> , BAST, BBIL, BALB, CYP3A, sex, BPBL, solid tumor, race, combination therapy with chemotherapeutic agents
Vc/F	Sex, BALB, BPBL, solid tumor, combination therapy with chemotherapeutic agents
Vp/F	BALB, BPBL, solid tumor, combination therapy with chemotherapeutic agents
Q/F	Solid tumor, combination therapy with chemotherapeutic agents
k <sub>a</sub>	Formulation, combination therapy with chemotherapeutic agents

Age indicates baseline age; BALB, baseline albumin; BAST, baseline aspartate aminotransferase; BBIL, baseline total bilirubin; BCCL<sub>i</sub>, baseline creatinine clearance for the *i*-th individual; BPBL, baseline percentage blasts in bone marrow; BWT<sub>i</sub>, baseline body weight for the *i*-th individual; CL/F, apparent total clearance; CYP3A, use of concomitant cytochrome P450 3A moderate or strong inhibitor; k<sub>a</sub>, first-order absorption rate constant; PK, pharmacokinetic; Q/F, intercompartmental clearance; Vc/F, central volume of distribution; Vp/F, peripheral volume of distribution; WNCL<sub>i</sub>, baseline standardized creatinine clearance for the *i*-th individual.

<sup>a</sup>WNCL<sub>i</sub> = BCCL<sub>i</sub> × 70/BWT<sub>i</sub>

percentage bone marrow blasts), use of a moderate or strong CYP3A inhibitor, tumor type (hematologic malignancy or solid tumor), and pharmaceutical formulation were evaluated (Table 1). The covariates were screened for pairwise correlation, and the more clinically relevant covariate or the one with greater statistical significance was selected to be included in the model (Supplemental Figure S1).

Categorical covariates were included using a linear model. Continuous covariates were included using a linear or power model. If a baseline continuous covariate value was found to be missing and the covariate was measured at postbaseline visits, that value was then imputed using the value at the first available, or earliest, postbaseline visit. If a continuous covariate value was entirely missing for the patient, the baseline value was imputed as the population median baseline value.

### Model Evaluation

At all stages of model development, goodness of fit was evaluated using the following criteria: OFV, condition number, visual inspection of different diagnostic plots, precision of the parameter estimates, and decreases in IIV and residual variability.

Diagnostic plots were examined to assess model adequacy, possible lack of fit, or violation of assumptions. Prediction-based plots of observed values versus Monte Carlo-generated population predictions and observed values versus individual predictions were evaluated for randomness around the line of unity. Residual-based diagnostic plots of conditional weighted and individual weighted residuals versus time

and model predicted values were evaluated for randomness around the 0 line. Empirical Bayes estimates (EBEs)-based diagnostics were also performed, thus, the distribution of  $\eta$ s was checked to ensure approximately normal distribution. In addition, plots of  $\eta$ s in the final model versus each covariate were compared with similar plots for the base model to demonstrate that the final model accounted for trends observed with the base model.

Both  $\eta$ -shrinkage (1 standard deviation [ $\eta$ EBE]/ $\omega$ ) and  $\epsilon$ -shrinkage (1 SD [individual weighted residuals]) were evaluated to assess the validity of using post hoc individual parameter estimates for model diagnosis.<sup>14</sup>

Nonparametric resampling (bootstrap) was carried forward to calculate CIs of the estimated PK parameters because the working assumption is that observations in a data set differ randomly, and it is this random difference that gives rise to the uncertainty in a parameter. All postprocessing graphical and statistical analyses were completed with R version 3.2.2 (R Foundation for Statistical Computing, Vienna, Austria).

The performance of the final model was evaluated by simulation-based diagnostics of the final data set using the parameter estimates from the final model (fixed and random effects) and conducting a visual predictive check (VPC).<sup>13,14</sup> However, the diagnostic value of the VPC could be hampered by binning across a large variability in dose and/or influential covariates. The prediction-corrected VPC offers a solution to these problems while it retains the visual interpretation of the traditional VPC. In the prediction-corrected VPC, the variability coming from binning across independent variables is removed by normalizing the observed and simulated dependent variable based on the typical population prediction for the median independent variable in the bin. Simulations were performed using patients' characteristics as well as sampling history from the data set. The concentration-time data were summarized using the median and 5th and 95th percentiles. The study was used to stratify and summarize simulated and observed data. The concordance between individual observations and simulated values, as well as the distribution of observed and simulated data, were evaluated.

## Results

### Summary of Observed Data

Demographic and baseline data from 272 patients with various hematologic or solid tumor malignancies from the 3 clinical studies are summarized in Table 2. The evaluated dose levels ranged from 5 to 640 mg QD (Supplemental Table S3); the majority of patients received the clinical dose of 100 mg QD ( $n = 187$  [69%]). The median baseline age and weight of the patients were 69 years and 78.6 kg, respectively, and

**Table 2.** Patient Demographics and Baseline Characteristics by Study

	Study			
	B1371001 n = 47	B1371002 n = 23	B1371003 n = 202	All N = 272
	Population			
	Hematologic Malignancies	Solid Tumor Malignancies	AML or High-Risk MDS	All Patients
Age, y	69 (25, 89)	61 (27, 76)	70.5 (27, 92)	69 (25, 92)
Weight, kg	71.8 (43.5, 117.3)	73.8 (47.0, 127.4)	80.2 (47.5, 145.6)	78.6 (43.5, 145.6)
Male/Female, n	28/19	14/9	139/63	181/91
Race/ethnicity, n				
White	38	18	179	235
Black	4	0	12	16
Asian	1	3	5	9
Hispanic	2	2	5	11
Other	0	0	1	1
WBC, 10 <sup>9</sup> cells/L <sup>a</sup>	4.4 (0.4, 48.5)	6.5 (2.4, 11.6)	2.8 (0.4, 5850.0)	3.6 (0.4, 5850.0)
Percentage bone marrow blasts <sup>a</sup>	37 (0, 100)	Not applicable	39.5 (10, 100)	39.3 (0, 100)
Albumin, g/dL <sup>a</sup>	3.8 (2.4, 4.9)	4.1 (2.6, 4.6)	3.6 (0, 33.0)	3.7 (0, 33.0)
AST, U/L <sup>a</sup>	20.0 (10, 364)	23.5 (8, 150)	21.0 (8, 107)	21.0 (8, 364)
Bilirubin, mg/dL <sup>a</sup>	0.5 (0.1, 4.2)	0.6 (0.3, 1.8)	0.6 (0.02, 2.3)	0.6 (0.02, 4.2)
Hepatic function, n				
Normal (A)	39	16	165	220
Mild (B1)	4	3	19	26
Mild (B2)	3	3	11	17
Moderate (C)	0	0	3	3
Severe (D)	1	0	0	1
Missing	0	1	4	5
CR <sub>CL</sub> , mL/min <sup>a</sup>	86.1 (38.6, 224.8)	94.3 (46.6, 149.0)	78.2 (31.4, 238.4)	80.9 (31.4, 238.4)
Renal function, n				
Normal (A)	21	15	70	106
Mild (B)	22	3	78	103
Moderate (C)	4	4	54	62
Severe (D)	0	0	0	0
Missing	0	1	0	1
CYP3A inhibitor, n <sup>b</sup>				
None	32	21	101	154
Moderate	8	2	52	62
Strong	7	0	49	56

AML, acute myeloid leukemia; AST, aspartate transaminase; CR<sub>CL</sub>, creatinine clearance; CYP3A, cytochrome P450 3A; MDS, myelodysplastic syndrome; WBC, white blood cells.

The data presented are median (minimum, maximum) unless otherwise noted.

<sup>a</sup>The following variables had missing baseline values (n, %): albumin (4, 1.5%), AST (5, 1.8%), bilirubin (1, 0.4%), CR<sub>CL</sub> (1, 0.4%), percentage bone marrow blasts (19, 7.6%), WBC (1, 0.4%). The percentage missing calculation for the percentage bone marrow blasts variable was based on hematologic patients only.

<sup>b</sup>For CYP3A moderate or strong inhibitor use, 1 record per patient, that with the most extreme case, was considered in the summary (ie, if a patient reported use of both moderate and strong CYP3A inhibitor use, only the strong was considered).

the majority of patients were male (n = 181 [67%]). The median baseline CR<sub>CL</sub> (based on the Cockcroft-Gault equation) was 80.9 mL/min, and the number of patients with normal renal function or mild renal impairment (as defined by Kidney Disease Outcomes Quality Initiative classification<sup>15</sup>) were well matched at 39% and 38%, respectively; 62 (23%) patients had moderate renal impairment. Most patients had normal hepatic function (n = 220 [81%]), 43 (16%) had mild impairment, 3 (1%) had moderate impairment, and 1 had severe impairment (as defined by National Cancer Institute Organ Dysfunction Working Group criteria<sup>16</sup>).

### Base Model

The population PK analysis included 246 patients with hematologic malignancies and 23 with solid tumors (3 patients who did not have glasdegib PK concentrations were excluded), with 3616 glasdegib concentration data points.

In exploratory analyses it was determined that the 2-compartment model significantly improved model fit and reduced OFV compared with a 1-compartment model. Additional models evaluating absorption were tested, including addition of lag time, mixed 0- and first-order absorption, and transit compartment absorption. All of these models failed to improve model stability

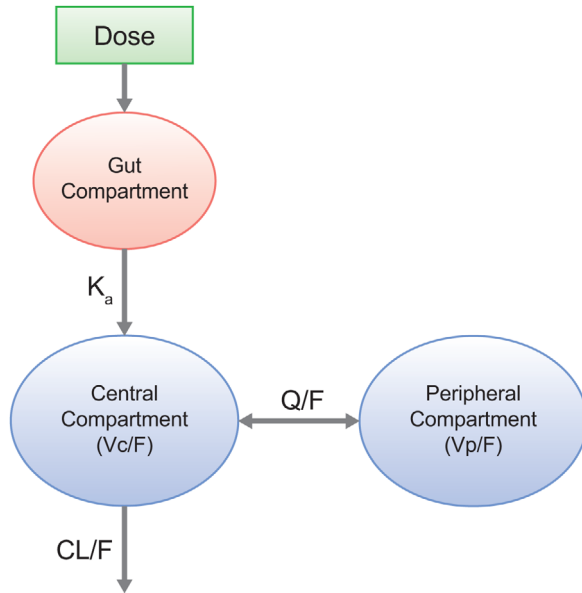


**Figure 1.** Two-compartment first-order absorption model. CL/F indicates apparent oral clearance;  $k_a$ , first-order absorption rate constant; Q/F, apparent intercompartmental clearance;  $V_c/F$ , apparent central volume of distribution;  $V_p/F$ , apparent peripheral volume of distribution.

(defined as condition number <1000), increased OFV, or showed significant bias in the prediction-based and residual-based diagnostic plots. (See Supplemental Table S4 for additional details of model development.) Therefore, the 2-compartment, first-order absorption model was determined to be the most appropriate structural model to characterize glasdegib PK (Figure 1).

Addition of allometric scaling of baseline body weight to the 2-compartment model with a scaling factor of 0.75 on CL/F and Q/F and 1.0 on  $V_c/F$  and  $V_p/F$  helped improve model stability and the diagnostic  $\eta$  versus covariate plots for baseline body weight and sex. Different error models were explored, and inclusion of 2 thetarized residual proportional errors separately for hematology and solid tumor patients resulted in statistically significant reduction in OFV and improvement in model stability. The final base model was a 2-compartment, first-order absorption model with allometric weight scaling and 2 thetarized residual error terms based on tumor type. The PK parameters from the base model are presented in Supplementary Table S5.

#### Covariate Analyses and Final Model

In the full model, baseline percentage bone marrow blasts, weight-standardized  $CR_{CL}$ , and use of moderate or strong CYP3A inhibitors were significant covariates on glasdegib CL/F ( $\alpha = 0.05$ ). Solid tumor malignancy was a significant covariate on  $V_p/F$  and Q/F. In the backward elimination step, all of the covariates from the full model were retained ( $\alpha = 0.001$ ).

The PK parameters from the final model are presented in Table 3. The typical value of CL/F is 6.27 L/h, with baseline body weight, weight-standardized  $CR_{CL}$ , percentage bone marrow blasts, and use of moderate or strong concomitant CYP3A inhibitors as predictors of IIV. The typical values of  $V_c/F$  and  $V_p/F$  were 3.32 L and 279.21 L, respectively, with body-weight scaling and tumor type as covariates. The typical value of Q/F was 1.288 L/h with allometric body weight scaling and tumor type as covariates. The typical value of  $k_a$  was estimated to be 0.06 hour<sup>-1</sup>. Inclusion of the covariates resulted in reduction in the coefficient of variation for  $\omega^2$ . The equations describing CL/F,  $V_c/F$ ,  $V_p/F$ , and Q/F parameters for the *i*-th individual are listed below:

$$CL/F_i = 6.27 \times \left(\frac{BWT}{70}\right)^{0.75} \times (1 - 0.173 \cdot CYP_{\text{moderate}}) \times (1 - 0.303 \cdot CYP_{\text{strong}}) \times \left(\frac{WNCL}{71.23}\right)^{0.406} \times (1 - 0.004 (BPBL - 38.20))$$

$$V_c/F_i = 3.32 \times \left(\frac{BWT}{70}\right)^1$$

$$V_p/F_i = 279.21 \times \left(\frac{BWT}{70}\right)^1 \times (1 - 0.825 \cdot \text{Solid})$$

$$Q/F_i = 1.29 \times \left(\frac{BWT}{70}\right)^{0.75} \times (1 - 0.653 \cdot \text{Solid})$$

wherein BPBL is baseline percentage bone marrow blasts, BWT is baseline body weight, and WNCL is weight-standardized  $CR_{CL}$ . In line with other oral oncology drugs, the residual variability for both hematologic and solid tumor patients was around 60% to 70% despite inclusion of covariates.<sup>17–21</sup>

Prediction-based diagnostic plots showed good agreement between model predictions and observed concentrations (Figure 2, Supplemental Figure S2). The final model described the data without any obvious bias in residual error over time and concentration (Figure 2). There were some data points (8 out of 3616 observations) identified as potential outliers using the criteria of absolute value of conditional weighted residuals or absolute value of individual weighted residuals > 6. After exclusion of these data points from the final model, the key parameter estimates did not change by more than 15%. Therefore, the outliers were not considered to be influential on the key parameter estimates and were retained.

**Table 3.** Final Model and Bootstrap Parameter Estimates

	Final Model					Healthy Volunteer Model <sup>b</sup>
	Estimate <sup>a</sup>	RSE (%)	Shrinkage (%)	Bootstrap (Median)	Bootstrap 95%CI	
OFV		1471.574				83.523
CL/F, L/h	6.27	6.4	–	6.23	5.56 to 6.81	10.1 (4.1%)
$\theta$ CYP <sub>mod</sub>	–0.17	59.4	–	–0.18	–0.37 to 0.09	
$\theta$ CYP <sub>strong</sub>	–0.30	36.6	–	–0.31	–0.53 to –0.06	
$\theta$ WNCL	0.41	23.3	–	0.41	0.22 to 0.60	
$\theta$ BPBL	–0.004	34.5	–	–0.004	–0.006 to –0.001	
V <sub>c</sub> /F, L	3.32	23.7	–	3.52	1.87 to 5.55	112 (4.1%)
V <sub>p</sub> /F, L	279.21	90.0	–	296.04	80.09 to 1090.45	53.5 (6.9%)
$\theta$ solid	–0.825	14.6	–	–0.81	–0.95 to –0.30	
Q/F, L/h	1.29	46.6	–	1.58	0.90 to 2.57	1.92 (11.4%)
$\theta$ solid	–0.65	24.4	–	–0.69	–0.91 to –0.27	
k <sub>a</sub> , hour <sup>–1</sup>	0.06	5.0	–	0.06	0.06 to 0.07	0.79 (8.9%)
Intersubject variability						
CL/F	43.0%	14.8	16.2	42.3%	36.8% to 49.4%	19.6% (5.8%)
V <sub>c</sub> /F	215.3%	22.8	22.6	215.2%	170.3% to 267.6%	11.0% (52.0%)
V <sub>p</sub> /F	112.8%	118.9	69.1	126.8%	42.4% to 212.8%	3.2% FIXED
Q/F	65.8%	36.3	62.9	59.7%	18.0% to 85.8%	3.2% FIXED
k <sub>a</sub>	13.5%	97.8	70.7	11.0%	4.1% to 21.1%	53.4% (10.6%)
Residual error, proportional error						
Hematologic	65.8%	5.2	–	65.7%	59.2 to 73.3	58.6%
Solid tumors	59.5%	7.0	–	59.3%	51.4 to 67.9	

BPBL, baseline percentage bone marrow blasts; CL/F, apparent clearance; CV, coefficient of variation; CYP<sub>mod</sub>, use of concomitant moderate cytochrome P450 3A inhibitor; CYP<sub>strong</sub>, use of concomitant strong cytochrome P450 3A inhibitor; FOCEL, first-order conditional estimation with interaction; k<sub>a</sub>, first-order absorption rate constant; OFV, objective function value; Q/F, intercompartmental clearance; RSE, relative standard error; solid, patients with solid tumor; V<sub>c</sub>/F, apparent central volume of distribution; V<sub>p</sub>/F, apparent peripheral volume of distribution; WNCL, baseline standardized creatinine clearance.

The median and 95%CI are generated from a bootstrap run of 1000 resampled data sets.

<sup>a</sup>Model estimates are typical  $\theta$  values. For intersubject variability, estimates are CV (%).

<sup>b</sup>The healthy volunteer model included noncancer subjects from studies B1371010 and B1371014 (n = 49; 1937 concentrations) and was described by a 2-compartment model with allometric body weight scaling and first-order absorption and elimination. FOCEL was the estimation method used. Food was empirically added as a covariate on k<sub>a</sub> by linear function. Residual error was described by proportional error model of all subjects.

Prediction-corrected VPC plots demonstrated that the final model could reasonably describe the central tendency and variability of glasdegib PK, thus suggesting lack of model misspecification (Figure 3). Bootstrapping was based on 1000 resampled data sets. All final model estimates were similar to the median values of the bootstrap estimates and were within the 95%CI. Of note, the 95%CI of the bootstrap estimate for use of moderate CYP3A inhibitor on CL/F encompassed 0. Bootstrap 95%CI estimates for all other covariate parameters excluded 0.

Exploratory modeling suggested the healthy volunteer population may exhibit different glasdegib PK from the cancer patient population. The parameter estimates from a 2-compartment, first-order absorption model using data from the healthy volunteer studies B1371010 and B1371014 are also presented in Table 3 as a comparison to the final model estimates based on the pooled data from patients with cancer. Glasdegib CL/F estimates for healthy subjects were >1.6-fold higher than in patients with cancer.

### Effect of Covariates

For a typical 70-kg patient with hematologic malignancy, 38.2% bone marrow blasts (population median), and no concomitant use of a CYP3A inhibitor, glasdegib CL/F is estimated at 6.27 L/h, V<sub>c</sub>/F at 3.32 L, V<sub>p</sub>/F at 279.21 L, and Q/F at 1.29 L/h. The impact of the significant covariates in the final model is presented in Table 4. Demographic and baseline characteristics, such as sex, age, race, and hepatic function, were not found to have an effect on glasdegib PK. A simulation using final model parameters (n = 500) was conducted to evaluate the change in steady-state exposure (maximum concentration and area under the concentration-time curve) for the significant covariates (Figure 4).

**Body Weight.** Body weight was included on clearance parameters (CL/F and Q/F) as a fixed effect using the scaling exponent of 0.75, and on the volume of distribution parameters (V<sub>c</sub>/F and V<sub>p</sub>/F) with a scaling exponent of 1. At the 10th percentile baseline body weight (61.2 kg) as compared with a typical 70-kg

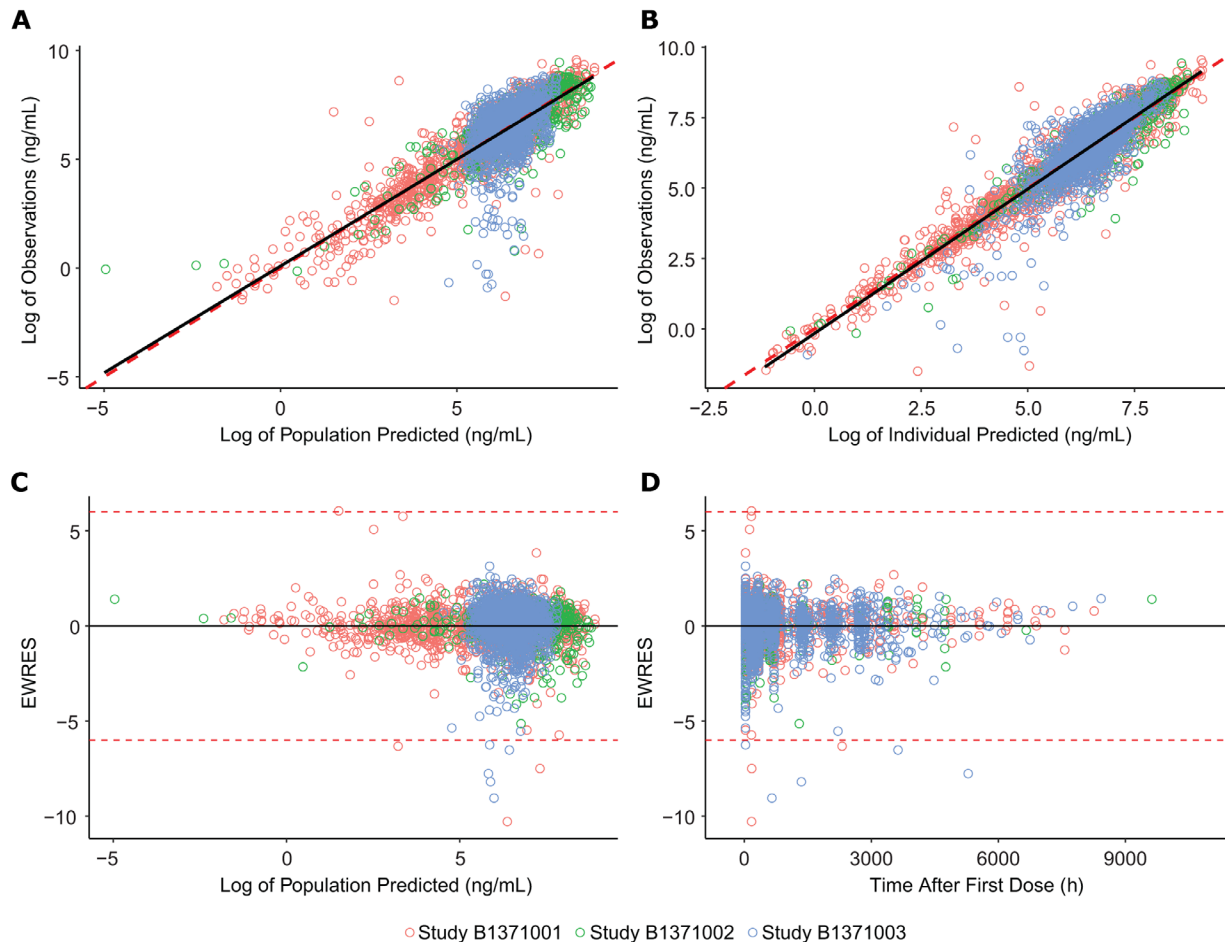


**Figure 2.** Prediction- and residual-based goodness-of-fit diagnostic plots. Prediction-based diagnostic goodness-of-fit plots by study of logarithm of observed glasdegib concentration versus (A) logarithm of EPRED and (B) IPRED concentrations. Dashed line represents line of unity, and solid line represents linear smooth line. Residual-based diagnostic goodness-of-fit plots of EWRES vs (C) logarithm of EPRED concentration and (D) time after first dose. Dashed lines (C and D) are at  $EWRES = -6$  and  $EWRES = 6$ . EPRED indicates population predicted; EWRES, conditional weighted residual; IPRED, individual predicted; log, natural logarithm transformed.

patient, there was a 10% and 13% decrease in glasdegib CL/F and Vc/F, respectively. At the 90th percentile body weight (102.1 kg), there was a 33% and 46% increase in CL/F and Vc/F, respectively, compared with a 70-kg patient.

**Bone Marrow Blasts at Baseline.** The final model suggested that a 1% change in baseline percentage bone marrow blasts from the population median value of 38.2% would result in an estimated 0.4% change in glasdegib CL/F. Relative to the median, a patient in the 10th percentile with 15% baseline bone marrow blasts had an ~9% increase in glasdegib CL/F. In contrast, a patient in the 90th percentile with 83% baseline bone marrow blasts had 17% reduction in glasdegib clearance.

**Concomitant Use of CYP3A Inhibitors.** In study B1371003, >40% of patients reported use of a

moderate and/or strong CYP3A inhibitor with glasdegib (Table 2). Concomitant use of a moderate or strong CYP3A inhibitor with glasdegib resulted in a 17% and 30% decrease, respectively, in glasdegib CL/F.

**Renal Impairment Status.** In the model, baseline weight-standardized  $CR_{CL}$  was evaluated instead of baseline  $CR_{CL}$  in order to avoid duplicate accounting of the effect of body weight on glasdegib CL/F (Table 1). Across the 3 clinical studies, the number of patients with normal renal function and mild renal impairment were well matched ( $n = 105$  and  $n = 102$ , respectively) with the median baseline weight-standardized  $CR_{CL}$  of 71.2 mL/min (81.0 mL/min for median baseline  $CR_{CL}$  as determined using the Cockcroft-Gault equation). For the patient with median  $CR_{CL}$  and normal renal function, weight-normalized glasdegib CL/F was estimated at 6.5 L/h. For the patient with median  $CR_{CL}$  and mild versus moderate renal impairment ( $n = 61$ ),

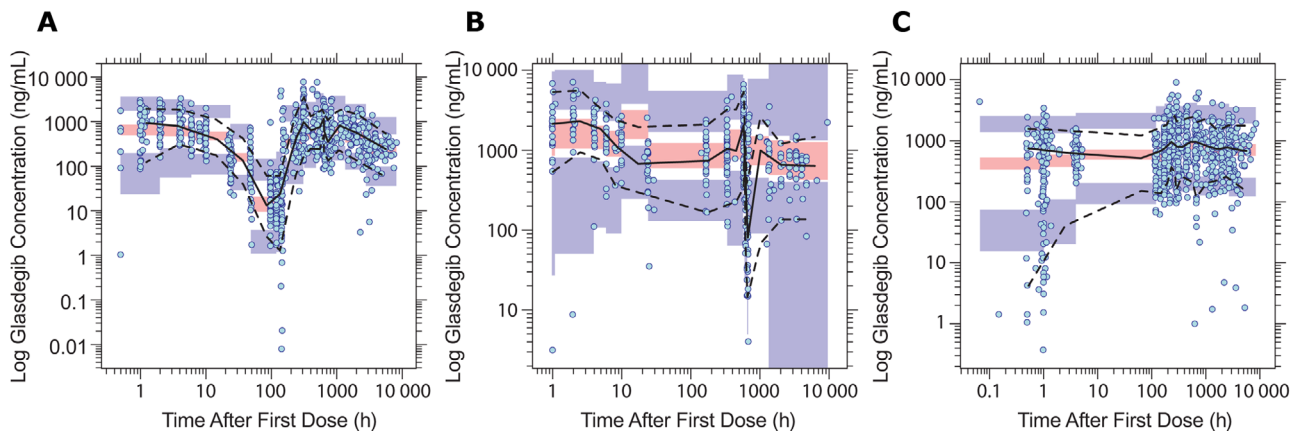


**Figure 3.** Prediction-corrected VPC by study. Prediction-corrected VPC of (A) study B1371001, (B) study B1371002, and (C) study B1371003. Shaded areas represent the 95% CIs of the predicted percentiles. Solid line represents the 50th percentile, and dashed lines represent the 5th and 95th percentiles. Observed data are represented by circles ( $\circ$ ). log indicates natural logarithm transformed; VPC, visual predictive check.

**Table 4.** Effect of Significant Covariates

Baseline Covariate	Group/Value (Percentile)	Parameter	Estimate	Change
Typical 70-kg hematologic patient with 38.2% BMB and no concomitant use of CYP3A inhibitor		CL/F, L/h	6.3	...
		Vc/F, L	3.3	
		Vp/F, L	279.2	
		Q/F, L/h	1.3	
Body weight	61.24 kg (10th)	CL/F, L/h	5.7	↓ 10%
		Vc/F, L	2.9	↓ 13%
	102.1 kg (90th)	CL/F, L/h	8.3	↑ 33%
Percent BMB	15% (10th)	Vc/F, L	4.8	↑ 46%
	83% (90th)	CL/F, L/h	6.9	↑ 9%
Use of CYP3A inhibitor	Moderate	CL/F, L/h	5.1	↓ 17%
	Strong	CL/F, L/h	5.2	↓ 17%
CR <sub>CL</sub> <sup>a</sup>	110.2 mL/min (normal)	CL/F, L/h <sup>b</sup>	4.4	↓ 30%
	75.5 mL/min (mild)		6.5	—
	51.1 mL/min (moderate)		6.2	↓ 5%
Tumor type	Solid tumor malignancy		4.8	↓ 26%
		Vp/F, L	48.9	↓ 83%
		Q/F, L/h	0.4	↓ 65%

BMB indicates bone marrow blast; CL/F, apparent total clearance; CR<sub>CL</sub>, creatinine clearance; CYP3A, cytochrome P450 3A; Q/F, apparent intercompartmental clearance; Vc/F, apparent central volume of distribution; Vp/F, apparent peripheral volume of distribution.

<sup>a</sup>Median baseline CR<sub>CL</sub> value for the respective renal impairment group is presented. CR<sub>CL</sub> is estimated by Cockcroft-Gault equation.

<sup>b</sup>The CL/F estimate for renal function is normalized by baseline body weight.

weight-normalized glasdegib CL/F was estimated at 6.2 L/h versus 4.8 L/h, respectively, representing a 26% decrease in CL/F in patients with moderate renal impairment as compared with normal renal function.

**Tumor Type.** Patients with solid tumor malignancies were examined relative to patients with hematologic malignancies and had ~83% and ~65% lower glasdegib Vp/F and Q/F, respectively.

## Discussion

The population model for glasdegib, a 2-compartment, first-order absorption model with allometric body-

weight scaling and thetarized proportional errors, adequately described the kinetic behavior of glasdegib in patients with hematologic and solid tumor malignancies. Demographic and baseline characteristics, such as age, sex, race, and hepatic function (Table 2), were evaluated but not found to be significant covariates on glasdegib PK parameters. The final model identified several covariates that were statistically significant and can explain some of the sources of variability in CL/F, Vp/F, and Q/F estimates.

Baseline body weight was added a priori to the model using allometric scaling on clearance (ie, CL/F and Q/F) and distribution (ie, Vc/F and Vp/F) parameters.



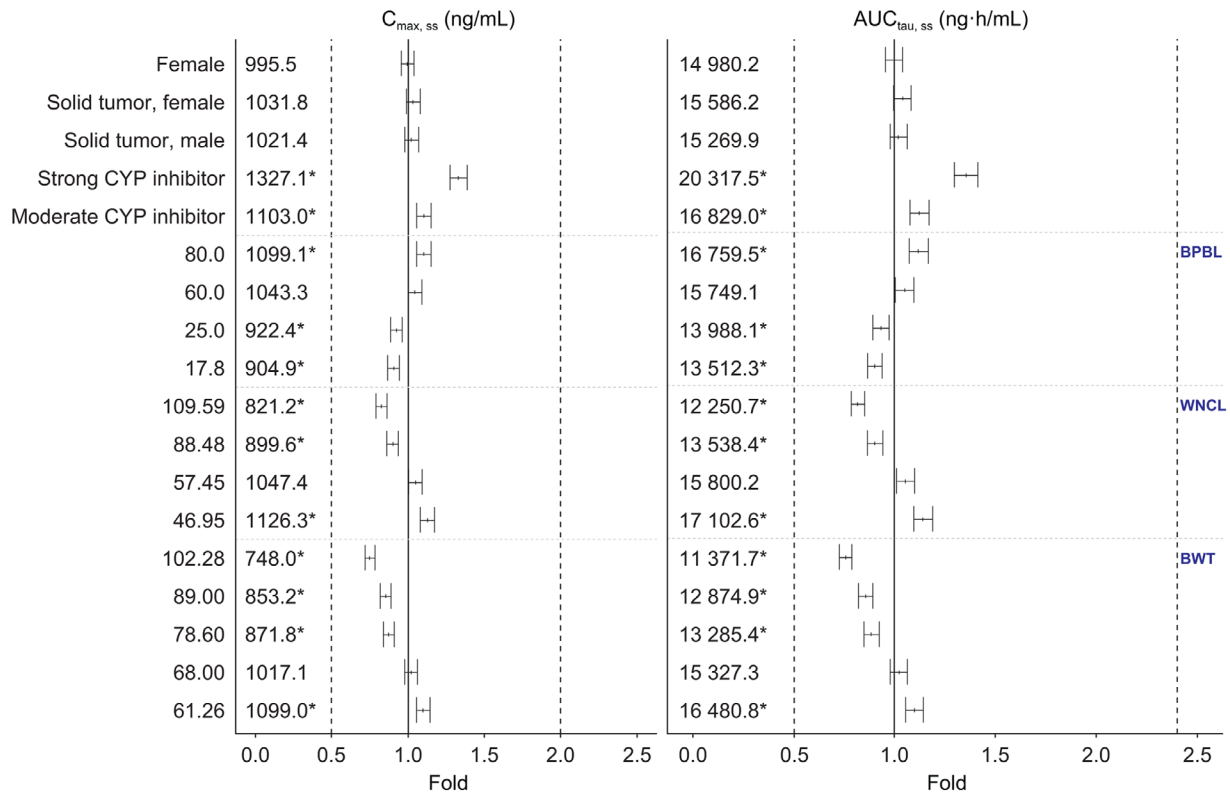


**Figure 4.** Forest plot of impact of significant covariates on glasdegib exposures. The median (point) and 90%CI for the fold change compared with the typical patient are presented for each scenario. The median pharmacokinetic parameter value ( $C_{max,ss}$  or  $AUC_{\tau,ss}$ ) for each scenario is also presented. The typical patient was considered a 70-kg male hematology patient, not taking concomitant CYP3A4 inhibitors, and with the median values for baseline weight, standardized creatinine clearance, and percentage bone marrow blasts. The typical patient is presented as the 1-fold solid black line. The dashed vertical lines represent the prespecified range of exposures over which no dose modification would be recommended. The values on the left of the y-axis represent the scenarios. The 10th, 25th, 75th, and 90th percentiles for BWT, WNCL, and BPBL are presented. For BWT, the 50th percentile is also presented. \*The difference in pharmacokinetic parameter value is statistically significant ( $\alpha = 0.01$ ) relative to the reference.  $AUC_{\tau,ss}$  indicates area under the concentration-time curve at steady state; BPBL, baseline percentage blasts in bone marrow; BWT, baseline body weight;  $C_{max,ss}$ , peak concentration at steady state; CYP, cytochrome P450; WNCL, weight-standardized  $CR_{CL}$ .

At the lower extreme of baseline body weight (ie, 10th percentile), the change in  $CL/F$  for a typical adult weight of 70 kg was a 10% reduction. This reduction in  $CL/F$  is not likely to result in a clinically meaningful exposure increase ( $\sim 1.1$  fold) that would warrant dose adjustment from a safety perspective, given that the MTD of glasdegib was 400 mg QD. At the high-extreme baseline body weight (ie, 90th percentile),  $CL/F$  is expected to increase by  $\sim 33\%$ , and the simulated fold change in steady-state maximum concentration and area under the curve is  $\sim 0.75$ , which will not pose additional safety risks and is not expected to result in a decrease in target modulation and hence reduced efficacy. Therefore, a dose adjustment from the clinical dose of 100 mg QD based on baseline body weight is not needed.

Determining the percentage of peripheral blood and bone marrow blasts is important in hematologic malignancies and is needed in diagnosing and characterizing the prognosis of patients with AML and MDS.<sup>22–24</sup> Bone marrow blasts  $>20\%$  generally confirm a diag-

nosis of AML.<sup>23</sup> It has previously been reported that leukemic blasts express SMO receptors.<sup>25</sup> Although the mechanism for this result is unknown, it may be hypothesized that patients with higher baseline percentage bone marrow blasts may express more targets for glasdegib binding, resulting in sequestration of glasdegib at the site of action and, therefore, reduced drug clearance. Among patients with hematologic malignancies in the data set (studies B1371001 and B1371003), the median baseline percentage of bone marrow blasts was 38.2%. Based on the results of the analysis, with every percentage increment of baseline bone marrow blasts over the population median value, there was a 0.4% decrease in glasdegib  $CL/F$ . However, given that the magnitude of glasdegib  $CL/F$  reduction at the upper extreme (ie, 90th percentile) is 17%, this is not likely to result in a clinically meaningful increase in exposure ( $\sim 1.1$  fold) and warrant dose adjustment due to safety.

Glasdegib is a substrate of CYP3A4 enzyme-mediated metabolism; thus, concomitant use of CYP3A inhibitors was evaluated for their impact

on glasdegib CL/F. In the clinical study in healthy subjects (B1371010), glasdegib as a 200-mg single dose was coadministered on day 4 of 7 continuous daily doses of ketoconazole 400 mg, a strong CYP3A inhibitor. Administration of glasdegib in the presence of ketoconazole resulted in a 140% higher area under the plasma concentration-time curve extrapolated to infinity and a 40% higher maximum plasma concentration compared with glasdegib administered alone.<sup>9</sup> This represents a decrease in glasdegib CL/F of 58% with ketoconazole. Across the 3 studies, over 40% of patients reported concomitant use of a moderate or strong CYP3A inhibitor with glasdegib treatment. The use of azole antifungal agents (also inhibitors of CYP3A) is common in patients with AML/MDS as clinically necessary interventions for treatment or prophylaxis of fungal infections. The population PK analysis estimated a 17% versus 30% reduction in CL/F with moderate versus strong CYP3A use. The magnitude of estimated decrease in glasdegib CL/F was less than the magnitude of decrease observed in the ketoconazole DDI study. According to clinical data of patients treated with glasdegib, the frequency and timing of dosing of CYP3A inhibitors plus glasdegib are likely not as well controlled as in the ketoconazole DDI study. Regardless, the 30% (or up to 58% with ketoconazole) decrease in glasdegib CL/F is not likely to pose additional safety risks due to the resultant increased glasdegib exposure (~1.4-fold in area under the curve for strong CYP3A inhibitors), given the clinical dose of 100 mg QD. In the first-in-patient dose-escalation study, the glasdegib MTD was determined to be 400 mg QD. Given that glasdegib exhibits linear PK, the MTD of 400 mg would translate to a 4-fold higher exposure compared with a clinical dose of 100 mg QD. The largest expected increase in glasdegib exposure due to the reduction in glasdegib CL/F with concomitant CYP3A inhibitor use is well below the expected exposure at the MTD.

Renal contribution to the elimination of glasdegib is around 17%, based on the results of a previously reported mass balance study.<sup>10</sup> Renal function classification for glasdegib-treated patients was based on the definitions of impairment by the National Kidney Foundation.<sup>15</sup> Across the 3 clinical studies, there were 105 (39%) patients with normal renal function, 102 (38%) with mild renal impairment, and 61 (23%) with moderate renal impairment. The median baseline  $CR_{CL}$  was 81.0 mL/min. Although baseline weight-standardized  $CR_{CL}$  was found to be a statistically significant covariate on glasdegib CL/F, post hoc estimates of decrease in glasdegib CL/F in patients with mild and moderate renal impairment were 5% and 26%,

respectively. The magnitudes of these findings are not clinically meaningful as to warrant dose adjustments for mild or moderate renal impairment. No patients in the clinical studies had severe renal impairment at baseline, and thus no conclusions could be drawn for this patient subpopulation.

Interestingly, patient population is an independent predictor of glasdegib PK variability, and this phenomenon appears to be a class-wide effect. In exploratory analyses with glasdegib PK data from healthy subjects, the estimated glasdegib CL/F was over 1.6-fold higher, and  $k_a$  was over 13-fold higher, than the final model estimates in pooled data from patients with hematologic and solid tumor malignancies. Sonidegib and vismodegib are 2 SMO inhibitors that have reported similar PK parameter differences. For sonidegib, the clearance was estimated to be 3-fold higher in healthy subjects than in patients with cancer.<sup>26</sup> The population PK model reported for vismodegib found close to doubling of  $k_a$  in healthy subjects versus oncology patients.<sup>27</sup> For glasdegib, a possible hypothesis that might explain the difference in clearance and volume of distribution estimates between healthy subjects and patients with cancer could be that there is a lower expression of SMO receptors in healthy subjects, although this has not been clinically evaluated. The covariate analysis for glasdegib found that patients with solid-tumor malignancies had ~83% and ~65% lower glasdegib Vp/F and Q/F, respectively, compared with patients with hematologic cancers. Currently, the mechanism for this is unknown. However, it can be hypothesized that patients with solid tumors lack high SMO-binding targets of leukemic blasts that are seen in patients with AML or MDS<sup>25</sup> and, therefore, have lower glasdegib target binding and distribution. The key parameters, CL/F and Vc/F, were not affected by tumor type, and glasdegib exposures are not expected to be different in patients with solid tumors.

At plasma exposures to glasdegib doses  $\geq 100$  mg QD, the downregulation of the Hedgehog pathway marker glioma-associated oncogene homolog 1 (GLI1) was robust and consistent, with no advantage for GLI1 modulation with higher doses compared with 100 mg QD.<sup>3</sup> The population PK model characterized the variability in glasdegib PK across the population through understanding the covariates that were significant and determining the clinical relevance of significant covariates. Subsequently, the individual post hoc estimates of glasdegib exposure metrics were derived from this population PK model in exposure-response analyses for efficacy and safety, which were instrumental in providing further justification for the recommended starting dose of 100 mg QD.<sup>28,29</sup>

## Conclusions

In conclusion, the population PK of glasdegib was well characterized by a 2-compartment model with first-order absorption. Covariates that were statistically significant in the analysis were not considered to change glasdegib PK in a clinically meaningful manner and did not warrant any changes to the recommended glasdegib dose of 100 mg QD.

## Funding

This study was funded by Pfizer.

## Medical Writing Support

Editorial support was provided by Sabrina Giavara and Gemma Shay of Engage Scientific Solutions and was funded by Pfizer.

## Conflicts of Interest

S.L., N.S., and A.R.G. are employees of Pfizer. G.M. has served as a consultant for Amgen, ARIAD, Incyte, Pfizer, Celgene, Janssen, Jazz, Daiichi Sankyo, and AbbVie; participated in speakers bureaus for Pfizer, Celgene, and Novartis; and has received research funding from Pfizer and AbbVie. A.J.W. has served as a consultant to Eli Lilly, Five Prime Therapeutics, and Daiichi Sankyo and has received research funding for his institution from Pfizer, Novartis, Eli Lilly, Five Prime Therapeutics, Daiichi Sankyo, Plexikon, Karyopharm, AADi, Merck, and Sanofi. J.C. has served as a consultant to Daiichi Sankyo, Novartis, Pfizer, and Astellas; research funding from Celgene, Sun Pharma, Daiichi Sankyo, Novartis, Pfizer, Astellas, and Arog; and holds stock options from Bio-Path Holdings.

## Author Contributions

S.L. and N.S. wrote the manuscript; N.S. designed the research; G.M., A.J.W., and J.C. performed the research; S.L. and A.R.G. analyzed data.

## Data Sharing

On request, and subject to certain criteria, conditions, and exceptions (see <https://www.pfizer.com/science/clinical-trials/trial-data-and-results> for more information), Pfizer will provide access to individual deidentified participant data from Pfizer-sponsored global interventional clinical studies conducted for medicines, vaccines, and medical devices (1) for indications that have been approved in the United States and/or European Union or (2) in programs that have been terminated (ie, development for all indications has been discontinued). Pfizer will also consider requests for the protocol, data dictionary, and statistical analysis plan. Data may be requested from Pfizer trials 24 months after study completion. The deidentified participant data will be made available to researchers whose proposals meet the research criteria and

other conditions, and for which an exception does not apply, via a secure portal. To gain access, data requestors must enter into a data access agreement with Pfizer.

## References

- Martinelli G, Oehler VG, Papayannidis C, et al. Treatment with PF-04449913, an oral smoothened antagonist, in patients with myeloid malignancies: a phase I safety and pharmacokinetics study. *Lancet Haematol*. 2015;2(8):e339-346.
- Wagner AJ, Messersmith WA, Shaik MN, et al. A phase I study of PF-04449913, an oral hedgehog inhibitor, in patients with advanced solid tumors. *Clin Cancer Res*. 2015;21(5):1044-1051.
- Minami Y, Minami H, Miyamoto T, et al. Phase I study of glasdegib (PF-04449913), an oral smoothened inhibitor, in Japanese patients with select hematologic malignancies. *Cancer Sci*. 2017;108(8):1628-1633.
- Savona MR, Pollyea DA, Stock W, et al. Phase Ib study of glasdegib, a Hedgehog pathway inhibitor, in combination with standard chemotherapy in patients with AML or high-risk MDS. *Clin Cancer Res*. 2018;24(10):2294-2303.
- Adis Insight. An open-label phase Ib study of PF-04449913 (glasdegib) in combination with azacitidine in patients with previously untreated higher-risk myelodysplastic syndrome, acute myeloid leukemia, or chronic myelomonocytic leukemia. <http://adisinsight.springer.com/trials/700254181>. Accessed November 8, 2018.
- Pfizer Inc. Daurismo (glasdegib) prescribing information. [https://www.accessdata.fda.gov/drugsatfda\\_docs/label/2018/210656s000lbl.pdf](https://www.accessdata.fda.gov/drugsatfda_docs/label/2018/210656s000lbl.pdf). Accessed February 27, 2019.
- Giri N, Lam LH, LaBadie RR, et al. Evaluation of the effect of new formulation, food, or a proton pump inhibitor on the relative bioavailability of the smoothened inhibitor glasdegib (PF-04449913) in healthy volunteers. *Cancer Chemother Pharmacol*. 2017;80(6):1249-1260.
- Shaik MN, Hee B, Wei H, LaBadie RR. Evaluation of the effect of rifampin on the pharmacokinetics of the Smoothened inhibitor glasdegib in healthy volunteers. *Br J Clin Pharmacol*. 2018;84(6):1346-1353.
- Shaik MN, LaBadie RR, Rudin D, Levin WJ. Evaluation of the effect of food and ketoconazole on the pharmacokinetics of the smoothened inhibitor PF-04449913 in healthy volunteers. *Cancer Chemother Pharmacol*. 2014;74(2):411-418.
- Lam JL, Vaz A, Hee B, Liang Y, Yang X, Shaik MN. Metabolism, excretion and pharmacokinetics of [<sup>14</sup>C]glasdegib (PF-04449913) in healthy volunteers following oral administration. *Xenobiotica*. 2017;47(12):1064-1076.
- Gibiensky L, Gibiinsky E, Bauer R. Comparison of Nonmem 7.2 estimation methods and parallel processing efficiency on a target-mediated drug disposition model. *J Pharmacokinetic Pharmacodyn*. 2012;39(1):17-35.
- Harling K, Hooker AC, Ueckert S, Jonsson EN, Karlsson MO. Perl speaks NONMEM (PsN) and Xpose. [https://www.page-meeting.org/pdf\\_assets/8110-PsN%20and%20Xpose%202011.pdf](https://www.page-meeting.org/pdf_assets/8110-PsN%20and%20Xpose%202011.pdf). Accessed November 8, 2018.
- Holford N. An introduction to visual predictive checks. <http://holford.fmhs.auckland.ac.nz/docs/vpc-tutorial-and-datatop.pdf>. Accessed November 8, 2018.
- Karlsson MO, Savic RM. Diagnosing model diagnostics. *Clin Pharmacol Ther*. 2007;82(1):17-20.
- Inker LA, Astor BC, Fox CH, et al. KDOQI US commentary on the 2012 KDIGO clinical practice guideline for the evaluation and management of CKD. *Am J Kidney Dis*. 2014;63(5):713-735.
- Patel H, Egorin MJ, Remick SC, et al. Comparison of Child-Pugh (CP) criteria and NCI organ dysfunction working

- group (NCI-ODWG) criteria for hepatic dysfunction (HD): implications for chemotherapy dosing. *J Clin Oncol*. 2004; 22(14\_suppl):1.
17. Tortorici MA, Cohen EE, Pithavala YK, et al. Pharmacokinetics of single-agent axitinib across multiple solid tumor types. *Cancer Chemother Pharmacol*. 2014;74(6):1279-1289.
  18. Golabchifar AA, Rezaee S, Dinan NM, Kebriaeezadeh A, Rouini MR. Population pharmacokinetic analysis of the oral absorption process and explaining intra-subject variability in plasma exposures of imatinib in healthy volunteers. *Eur J Drug Metab Pharmacokinet*. 2016;41(5):527-539.
  19. Hughes JH, Phelps MA, Upton RN, et al. Population pharmacokinetics of lenalidomide in patients with B-cell malignancies. *Br J Clin Pharmacol*. 2019;85(5): 924-934.
  20. Mei S, Li X, Jiang X, Yu K, Lin S, Zhao Z. Population pharmacokinetics of high-dose methotrexate in patients with primary central nervous system lymphoma. *J Pharm Sci*. 2018;107(5):1454-1460.
  21. Jain L, Woo S, Gardner ER, et al. Population pharmacokinetic analysis of sorafenib in patients with solid tumours. *Br J Clin Pharmacol*. 2011;72(2): 294-305.
  22. Montalban-Bravo G, Garcia-Manero G. Myelodysplastic syndromes: 2018 update on diagnosis, risk-stratification and management. *Am J Hematol*. 2018;93(1):129-147.
  23. DiNardo CD, Garcia-Manero G, Pierce S, et al. Interactions and relevance of blast percentage and treatment strategy among younger and older patients with acute myeloid leukemia (AML) and myelodysplastic syndrome (MDS). *Am J Hematol*. 2016;91(2):227-232.
  24. Amin HM, Yang Y, Shen Y, et al. Having a higher blast percentage in circulation than bone marrow: clinical implications in myelodysplastic syndrome and acute lymphoid and myeloid leukemias. *Leukemia*. 2005;19(9):1567-1572.
  25. Irvine DA, Copland M. Targeting Hedgehog in hematologic malignancy. *Blood*. 2012;119(10):2196-2204.
  26. Goel V, Hurh E, Stein A, et al. Population pharmacokinetics of sonidegib (LDE225), an oral inhibitor of hedgehog pathway signaling, in healthy subjects and in patients with advanced solid tumors. *Cancer Chemother Pharmacol*. 2016;77(4):745-755.
  27. Lu T, Wang B, Gao Y, Dresser M, Graham RA, Jin JY. Semi-mechanism-based population pharmacokinetic modeling of the Hedgehog pathway inhibitor vismodegib. *CPT Pharmacometrics Syst Pharmacol*. 2015;4(11):680-689.
  28. Ruiz-Garcia A, Shaik N, Jamieson C, Heuser M, Chan G. Pharmacokinetic/pharmacodynamic evaluation of the relationship between glasdegib exposure and safety endpoints in cancer patients. Presented at: American Association for Cancer Research; 110th Annual Meeting; April 2, 2019; Atlanta, Georgia. Poster 3887/7.
  29. Lin S, Shaik MN, Chan G, Cortes JE, Ruiz-Garcia A. Population pharmacokinetic/pharmacodynamic evaluation of the relationship between glasdegib treatment/exposure and overall survival in AML patients. *Blood*. 2018;132(suppl 1):1450.

### Supplemental Information

Additional supplemental information can be found by clicking the Supplements link in the PDF toolbar or the Supplemental Information section at the end of web-based version of this article.